



Combined mine tremors source location and error evaluation in the Lubin Copper Mine (Poland)

Andrzej Leśniak^{*}, Grzegorz Pszczoła¹

Department of Geoinformatics and Applied Computer Science, Faculty of Geology, Geophysics and Environmental Protection, AGH University of Science and Technology, Poland

Received 31 March 2006; accepted 24 April 2007

Abstract

A modified method of mine tremors location used in Lubin Copper Mine is presented in the paper. In mines where an intensive exploration is carried out a high accuracy source location technique is usually required. The effect of the flatness of the geophones array, complex geological structure of the rock mass and intense exploitation make the location results ambiguous in such mines. In the present paper an effective method of source location and location's error evaluations are presented, combining data from two different arrays of geophones. The first consists of uniaxial geophones spaced in the whole mine area. The second is installed in one of the mining panels and consists of triaxial geophones. The usage of the data obtained from triaxial geophones allows to increase the hypocenter vertical coordinate precision. The presented two-step location procedure combines standard location methods: P-waves directions and P-waves arrival times. Using computer simulations the efficiency of the created algorithm was tested. The designed algorithm is fully non-linear and was tested on the multilayered rock mass model of the Lubin Copper Mine, showing a computational better efficiency than the traditional P-wave arrival times location algorithm. In this paper we present the complete procedure that effectively solves the non-linear location problems, i.e. the mine tremor location and measurement of the error propagation.

© 2008 Elsevier B.V. All rights reserved.

Keywords: Mine tremors location; Non-linear optimization; Error estimation; Monte-Carlo methods

1. Introduction

Lubin Copper Mine (LCM) is an operating underground mine located in western part of Poland (see Fig. 1), mainly producing copper and silver. The average daily excavation is 21 thousand tones of ore and mining works are carried out at a depth of 610 to 850 m in nine working sections. Due to the firm, resistant rock mass and deep intense exploitation mine tremors frequently occur. In the case of LCM an accurate source location is required for rock mass instabilities prevention and efficient deposit management.

Tremors location in mines is an important and difficult task, especially when the coordinates of the seismic source need to be

determined with high accuracy. In Polish mines mine tremors are frequently located using the P-wave arrival times (Mendecki, 1997). In the case of LCM this algorithm turned out to be inadequate. Despite the fact that horizontal coordinates of the hypocenter were located well, the vertical coordinate was not. The computer simulations later described in this article confirm the large vertical coordinate location error, reaching an approximate value of about 400 m. For security and production planning reasons it was necessary to decrease the vertical location error of the mine tremors. In one of the mining panels at production level an additional, independent test array of the triaxial geophones was installed. Although it consisted of three triaxial geophones, it greatly increased the vertical accuracy of the located hypocenters.

The “traditional” linear P-wave arrival times algorithm used to locate tremors in mines is quite fast. Unfortunately, it can be easily applied for the simplest rock mass model: deterministic, homogeneous and isotropic medium. For application to more

^{*} Corresponding author. Tel.: +48 12 617 23 68; fax: +48 12 633 29 36.

E-mail addresses: lesniak@agh.edu.pl (A. Leśniak), gpszczoła@poczta.onet.pl (G. Pszczoła).

¹ Tel.: +48 503 314 390.

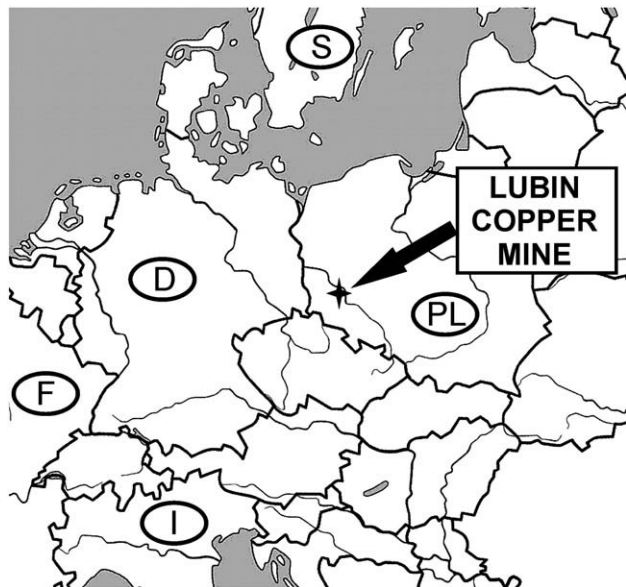


Fig. 1. Location of Lubin Copper Mine in Europe.

complicated rock mass models a non-linear version of this algorithm should be used. The use of the additional data obtained from triaxial geophones can rapidly decrease the computing time necessary to locate tremors and evaluate the location errors, allowing its application to more complex rock mass models. In the case of LCM the multilayer model was tested.

In order to check the accuracy of the newly created location procedure, an error estimation algorithm was designed based on multiple Monte-Carlo simulations. Unfortunately, the error maps evaluation is a time consuming procedure in such case, caused by large number of necessary simulations of location process. All the computations were performed in 30 nodes computer cluster, using parallel programming (C language and MPI library).

The primary objective of this paper was to develop an efficient method that increases the accuracy of the located hypocenters, especially regarding its vertical component. The method should also operate on the data provided from two independent arrays of geophones (uniaxial and triaxial). Furthermore, the efficiency of the developed algorithm should be checked by appropriate error estimation algorithm.

2. Mine tremor location algorithm

2.1. Location by P-wave first arrival times

From a typical mine tremor several different wave types are recorded by geophones array. For source location in mines the most common approach is to use only the P-waves, since it is easy for these waves to determine their exact first onset time on the seismogram. As the fastest wave in the rock mass, it reaches the geophones as the first one, therefore the first part of the signal is not disturbed by other waves and easy to extract. In the present work we have not used the other waves that can be used in source location (e.g. S shear wave). In multilayer media with

strong reflectors the S wave is overburdened by other shear waves generated at layers boundaries (for example converted waves generated by P-wave). Our mining experiences convinced us that determination of S wave onset in such cases can usually lead to problematic results.

The travel time of the P-wave depends on the source (hypocenter) location, the coordinates of the geophone and the P-wave velocity distribution in the rock mass. Let us assume that the hypocenter has approximate coordinates (x,y,z,t) and n is a number of geophones. The non-linear function that describes the misfit between observed and calculated arrival times is given by Eq. (1):

$$f(x, y, z, t) = \sum_{i=1}^n [t_i - t - T_i(x, y, z)]^2 \quad (1)$$

where T_i denotes the evaluated travel time of the P-wave from point (x,y,z) to the i -th geophone and t_i are the recorded P-wave arrival times detected at the i -th geophone.

During the evaluation of the function (1) the problem of determination of the P-wave ray path between point (x,y,z) and the geophone (x_i, y_i, z_i) arises. The solution for the horizontally stratified medium is described in Lee and Stewart (1981).

Function (1) has several properties:

- The global minimum of f is equal to zero if there are no measurement errors of the P-wave arrival times t_i and the used rock mass model fits real one,
- The global minimum points out the real hypocenter coordinates (x_0, y_0, z_0, t_0) .

The four parameters (x,y,z,t) can be reduced to three (x,y,z) by a procedure known as centering (Mendecki, 1997; Pavlis et al., 2004). The problem of finding the global minimum of f is usually solved by linearization of the function (1). In case of the multilayered medium the evaluations of $T_i(x,y,z)$ cannot be done analytically. Also, it is not easy to linearize f , often contains a large number of local minima in the case of complex environments (Pszczola and Leśniak, 2004).

The well known grid search algorithm (Pavlis et al., 2004) is often used in non-linear location problems. In case of LCM the standard grid search algorithm was replaced by Multistart (Horst and Pardalos, 1995) optimization technique. Multistart consists of two stages: At first, the point (x,y,z) is randomized. After that from the point (x,y,z) a local minimization procedure is launched. The results of the local minimizations are compared and the minimum with a minimal function (1) value is stored. After several iterations the global minimum of the function (1) will be found. For the local minimization algorithm the Powell conjugate directions (Press et al., 1986) method was used.

2.2. Location by the P-wave directions

As the P-wave is a longitudinal wave the triaxial geophone can record the direction (bearing and incidence angle) of the incoming wave. This direction, in case of the P-wave, can be easily determined by polarization analysis, as the principal

eigenvector of the covariance matrix at the P-wave onset — e.g. (Samson, 1977; Jurkasevics, 1988; Jackson et al., 1991; Wagner, Owens, 1996). That direction can also be extracted from its first breaks by approximation of the particle motion trajectory by a straight line, as was done in our case. The idea of the directional algorithm is presented in Fig. 2. For the best approximation of the hypocenter the minimum of the function (2) can be considered:

$$g(x, y, z) = \sum_{i=1}^N d_i(x, y, z) \quad (2)$$

where d_i denotes the distance from the point (x, y, z) to the i -th raypath and N is a number of triaxial geophones. The i -th raypath is obtained from the P-wave direction recorded by i -th geophone. The most time consuming part of the function (2) evaluation is the raytracing of all P-wave rays. As this can be computed only once during the whole minimization process, the minimization of Eq. (2) is much easier than Eq. (1). To minimize Eq. (2) the Multistart procedure was also used.

2.3. Combined algorithms

To constrain the location procedure we can merge the misfit functions given by Eqs. (1) and (2) to create a joint algorithm. In contrary to the described above procedures, the joint minimization that uses P-wave arrival times and P-wave directions can result in better source location, especially in low heterogeneous media. The effectiveness of the described location methods specified by error analysis will be presented in the next paragraph.

For joint algorithm the misfit function is a weighted combination of the misfit functions given by Eqs. (1) and (2):

$$h(x, y, z) = (1/n)(f(x, y, z)/\Sigma_t)^2 + (1/N)(g(x, y, z)/\Sigma_d)^2 \quad (3)$$

where Σ_t and Σ_d are, respectively, *a priori* estimates of the standard error of travel times and standard error of distances of each ray from the epicenter. As a result of such normalization

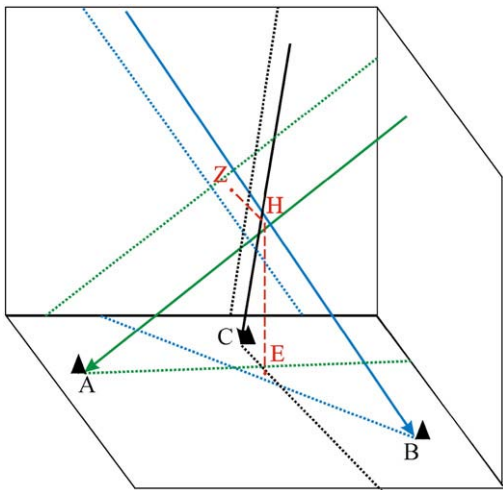


Fig. 2. The idea of the location by the P-wave directions. A, B, C — triaxial geophones, H — location of hypocenter, E — location of epicenter, Z — depth of hypocenter.

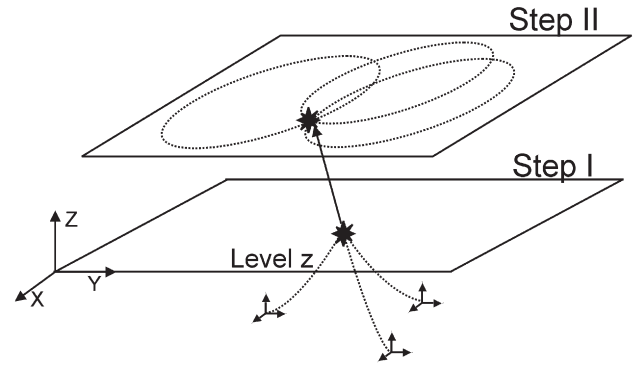


Fig. 3. Combined location algorithm. First step: from recorded P-wave directions the vertical coordinate of hypocenter is evaluated. Second step: to obtain the horizontal coordinates of the epicenter the P-wave arrival times algorithm is used.

we add dimensionless quantities of the same range. The values of Σ_t and Σ_d can be obtained using Monte-Carlo modeling method presented in the next chapter.

The detailed discussion of that procedure was presented e.g. by Mendecki (1997). To find the global minimum of the combined misfit function given in Eq. (3) the Multistart algorithm can be used. Although the location procedure is performed relatively quickly, the evaluation of location errors maps using Monte-Carlo simulation method is an extremely time consuming process.

An alternative idea of merging of both algorithms that allows to save computational time (in case of error computation) is presented in Fig. 3. Initially, the described above directional location algorithm is used. This stage is only applied to estimate the vertical coordinate of the located hypocenter. Then the P-wave arrival time algorithm is used. As the vertical coordinate of the located hypocenter is known, function (1) becomes three dimensional and depends only on three variables, x , y and t . We call this procedure “two-step algorithm”. Usually, the time consuming P-wave arrival time algorithm becomes faster and the “saved” computational time can be used to model more complex rock mass models. The evident virtue of the last method can be seen in Monte-Carlo modeling of the location errors presented below. Moreover, it is easy to create an efficient parallel computer code for such non-linear error estimation, what is crucial in solving industry-scale problems.

3. Error estimation algorithm

Errors of the source locations were estimated by a multiple Monte-Carlo modeling technique. For an hypothetical source located in point $p(x, y, z)$ (the (x, y, z) stands for coordinates of the particular point of the error map), the seismic rays to all sensors were modeled. For calculation we have used the stratified rock mass model with average velocity of the each layer perturbed by a random but systematic error (bias) σ_b and Gaussian error σ_v . The bias σ_b is constant inside each layer, while σ_v is variable inside each layer. For every seismic ray we evaluated the travel time and the incidence angle. To include the measurements error to the modeled rays we had to perturb the arrival times and

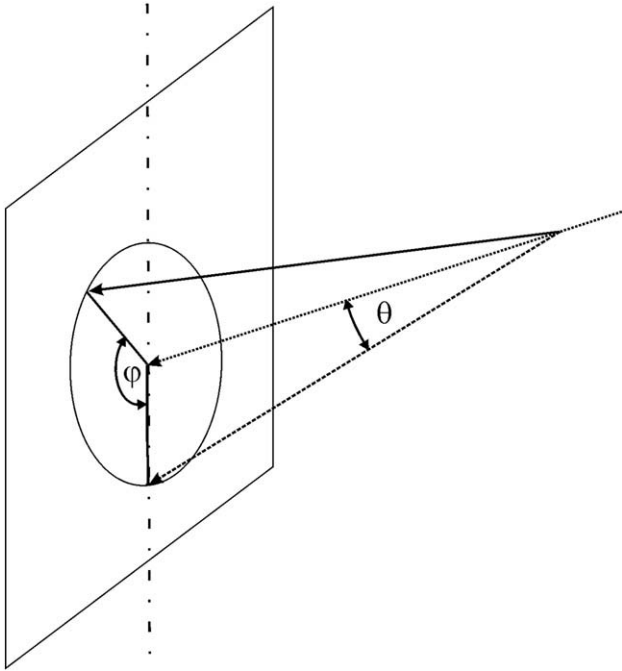


Fig. 4. Perturbation of the incidence direction of the seismic ray. The incidence vector (dotted line) is deflected by the random angle θ in the vertical direction. The resulted direction is shown as a dashed line vector. Then the incidence vector is rotated by angle φ around the no perturbed direction. The final direction is marked as a solid line vector.

incidence angles for all geophones. To carry out the first perturbation, a random number was added to the evaluated P-wave arrival times. It was drawn by the Gaussian random number generator with the mean value equal to zero and predefined standard deviation σ_r . The perturbation of the incidence angle was realized in two-step: First, the incidence vector of the seismic ray was deflected by the random angle θ in the vertical direction (Fig. 4). Then the incidence vector was rotated on angle φ around the no perturbed direction. The angles θ and φ were random numbers with Gaussian and uniform distributions respectively with mean values equal to zero and standard deviations equal σ_θ and σ_φ .

The observational errors ($\sigma_t, \sigma_\theta, \sigma_\varphi$) and the modeling errors (σ_b, σ_v) are used to evaluate the *a priori* estimates Σ_t and Σ_d necessary to perform joint location with penalty function given by Eq. (3). The estimate of the standard error of travel times Σ_t was evaluated as an averaged sum of squared differences between modeled propagation time and perturbed propagation time from each node to each geophone. Similarly, the standard error of distances of each ray from the epicenter Σ_d was evaluated as an averaged sum of squared differences of source-ray distances for unperturbed and perturbed rays for each node to each geophone.

Then the source coordinates $p'(x', y', z')$ were evaluated by an appropriate algorithm, described in paragraph 2 (the (x', y', z') stands for evaluated coordinates of the particular point of the error map). The tested algorithms were: location by P-wave first arrival times, location by P-wave directions and the both combined algorithms, i.e. the first one with combined misfit function and the second one — the two-step algorithm. The

difference between assumed $p(x, y, z)$ and evaluated $p'(x', y', z')$ source locations allow the estimation of the location error. After multiple modeling, adding noise and inverting, the location error for point (x, y, z) was estimated by the following estimators:

- Error estimator for epicenter (4):

$$\sigma_E = \sqrt{\frac{\sum_{i=1}^N (x_i' - x)^2 + (y_i' - y)^2}{N}} \quad (4)$$

- Error estimator for the depth coordinate (5):

$$\sigma_Z = \sqrt{\frac{\sum_{i=1}^N (z_i' - z)^2}{N}} \quad (5)$$

where (x, y, z) is the point at the map where the location error is evaluated (the assumed true hypocenter coordinates also), (x'_i, y'_i, z'_i) are the obtained (located) hypocenter coordinates at the i -th iteration, N , is the total number of the error algorithm iterations, σ_E , is the epicenter location error and σ_Z is the error of the vertical coordinate of the hypocenter.

4. Field example from LCM

The practical examples described below show the errors evaluations for all described methods of tremor locations. As a result of the presented analysis, we have chosen the two-step combined algorithm as a most suitable to locate strong tremors inside and near the mining panel G6/X/9, where triaxial geophones had been installed.

The seismic monitoring system used in LCM consisted of two independent arrays of different sensors. Small arrays consisted of three triaxial geophones located underground in mining panel, in shallow holes drilled in the roof. The sampling rate was 2 kHz and the digital transmission between geophones and the computer allowed to obtain the system dynamic range equal to 90 dB. The sampling rate of signals recorded by wide arrays of uniaxial geophones was equal to 0.5 kHz. The recorded signals were frequency modulated and then transmitted to the recording system placed in mine seismic office at the surface. The analogue transmission used in second array and moderate quality of the transmission network resulted in a lower dynamic range of the system equal to 65 dB.

In Fig. 5. the geophones location in LCM are presented. The uniaxial geophones are presented as dots, spaced all over the mine. The rectangle represents the area of the panel G6/X/9 at the production level, where it was necessary to increase the precision of the mine tremors location. Crosses in Fig. 5 show the array of the triaxial geophones installed in this mining panel. Due to the intense production at the panel G6/X/9 only three triaxial geophones were installed, as the maintenance of the greater geophones array at this panel would be technically very difficult.

The velocity model frequently used in the LCM mine for rough source location is homogeneous and isotropic, with a P-

wave velocity of 5800 m/s. Unfortunately this simple model for precise source location was inadequate. In our case for error evaluation the P-wave velocity model shown in Fig. 6 was used. The particular velocities have been laboratory measured on samples taken from the boreholes located in mining panel G6/X/9 by mining geologic survey.

To select the most appropriate method of tremors' location for the particular measurement setup of LCM we have modeled the errors of source locations. The location algorithm with the smallest location errors in the panel G6/X/9 was chose as a best one. The location errors maps were evaluated with Y varying between 9000 m and 11,000 m; X between 26,000 m and 27,900 m (panel G6/X/9) and Z set at -510 m (100 m above the production level at region where the three component sensors were installed). The number of evaluated points for each map was 10,000.

The measurement error was simulated in several ways:

- 1) The “ideal” directions recorded by triaxial geophones were deflected with the Gaussian distribution with standard deviation $\sigma_{\theta}=20^{\circ}$.
- 2) To evaluated P-wave arrival times the Gaussian noise was added with standard deviation $\sigma_t=10$ ms.
- 3) The varying velocity in the rock mass was modeled by adding to the velocities at each layer a Gaussian noise (standard deviation $\sigma_v=20\%$) and the bias equal to $\sigma_b=10\%$. Because bias is a systematic error, for each layer it was drawn only once for all error estimations, while the Gaussian error was

	1 800 m/s	Tertiary + Quaternary
350 m	3 600 m/s	Sandstone
25 m	3 200 m/s	Shale
151.4m	5 800 m/s	Anhydrite
4.6 m	4 500 m/s	Shale
22 m	5 800 m/s	Anhydrite
-605.7 m	5 800 m/s	Dolomite

Fig. 6. Simplified, 1-D P-wave velocity profile in the Lubin Copper Mine starting at level 610 m.

different in each point of the rock mass. The noise was added to the original rock mass model at each iteration of error estimation.

The following location algorithms were used: only first P-wave arrival times algorithm, P-wave directional algorithm and the both combined algorithms. Each of them used the Multistart procedure with a number of iterations equal to 100 to minimize

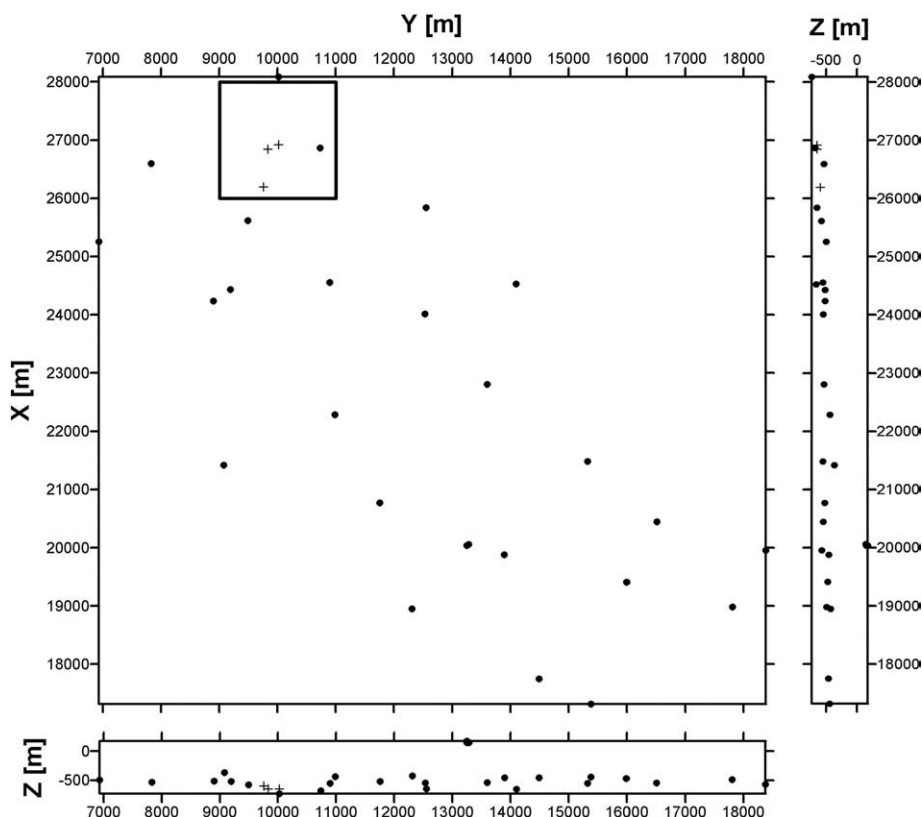


Fig. 5. Geophones location in Lubin Copper Mine. Dots — uniaxial geophones, crosses — triaxial geophones. Rectangle — the area where the accuracy of the mine tremors locations was necessary to be increased.

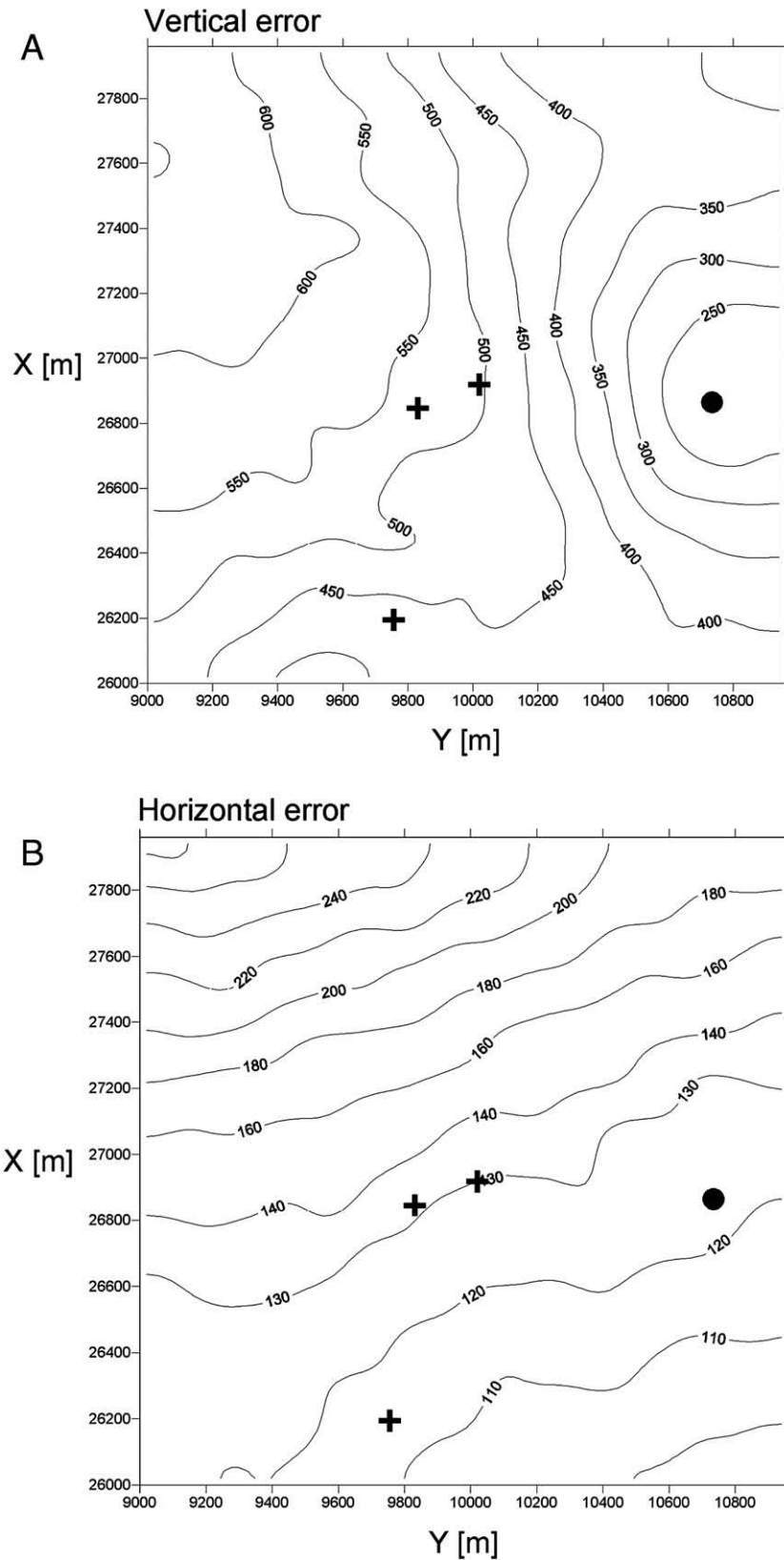


Fig. 7. Error of the location for the P-wave arrival times method: A) hypocenter vertical coordinate location error, B) epicenter error. Dot — uniaxial geophone, crosses — triaxial geophones.

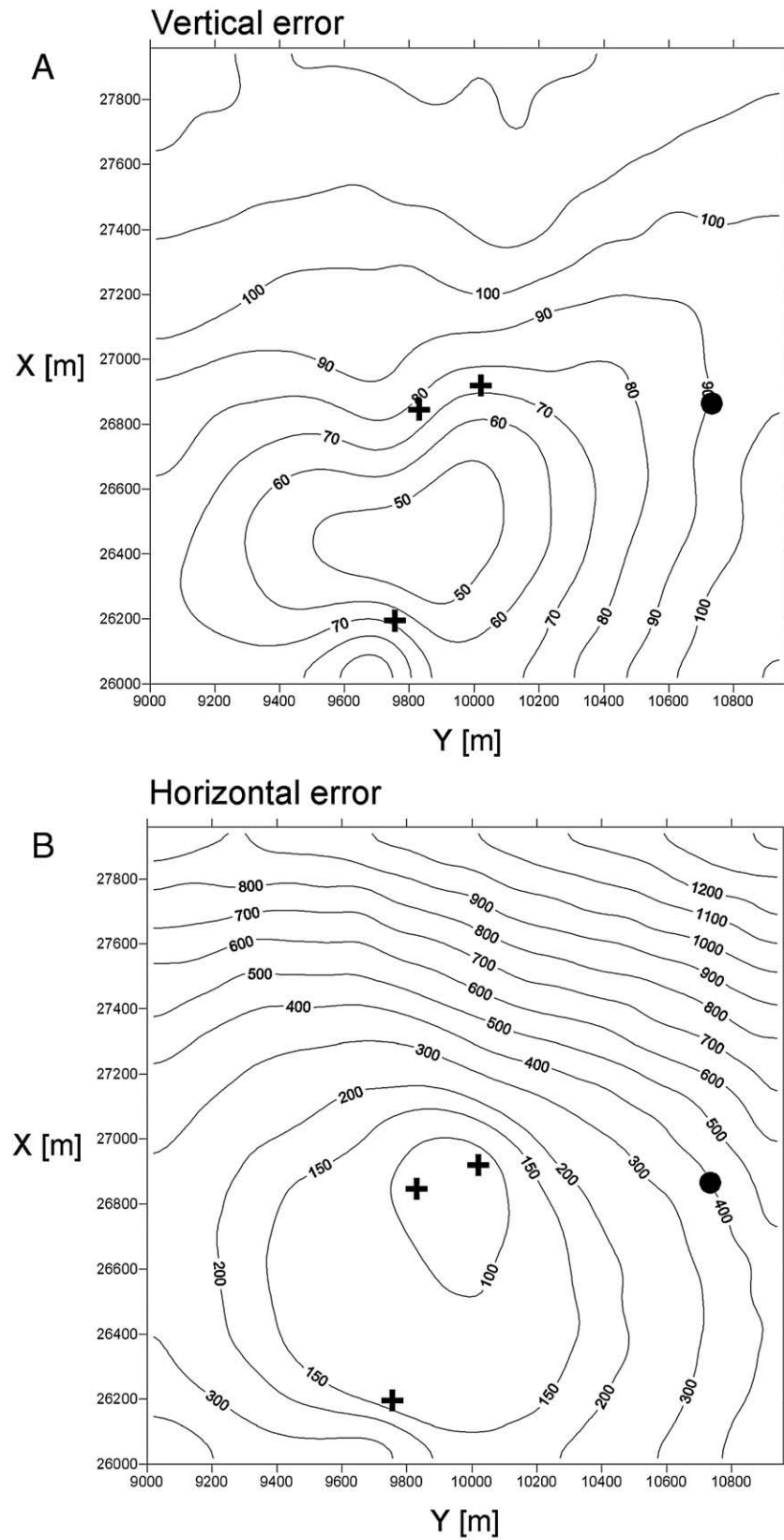


Fig. 8. Error of the location for the P-wave directional method: A) hypocenter vertical coordinate location error, B) epicenter error. Dot — uniaxial geophone, crosses — triaxial geophones.

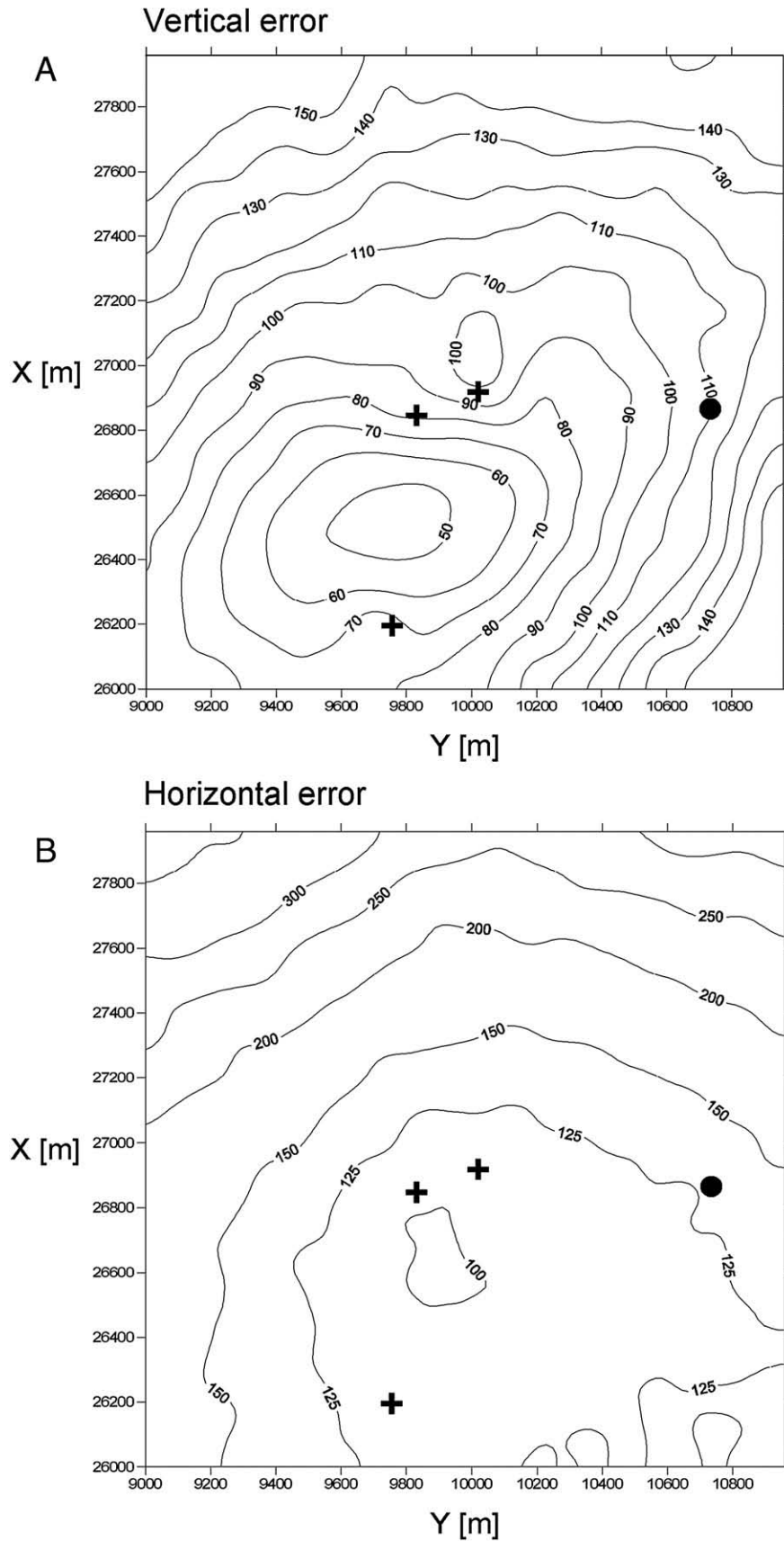


Fig. 9. Error of the location for the combined method with the joint misfit function. A) hypocenter vertical coordinate location error, B) epicenter error. Dot — uniaxial geophone, crosses — triaxial geophones.

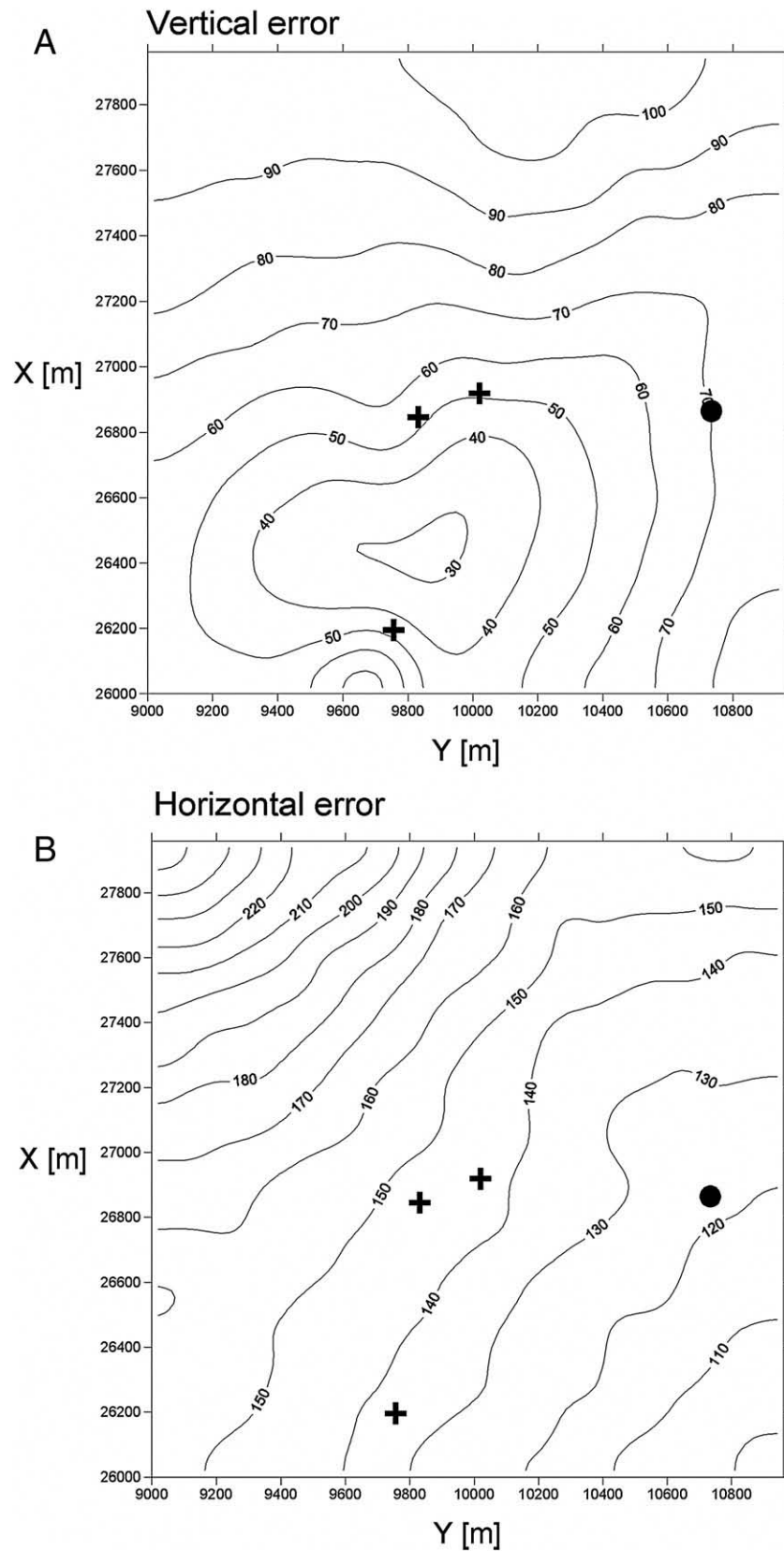


Fig. 10. Error of the location for the two-step combined method. A) hypocenter vertical coordinate location error, B) epicenter error. Dot — uniaxial geophone, crosses — triaxial geophones.

appropriate misfit function. The computations for the time consuming procedures (P-wave first arrival time and combined misfit function) and multilayered rock mass model were performed using a 30 nodes computer cluster for 15 h. For the two-step combined procedure the same computations took

only 1 h. All the programs were written in C and used parallel MPI library.

The errors maps constructed for the P-wave first arrival time algorithm (Fig. 7) shows that the method locates epicenters quite well (Fig. 7B). On the other hand, the vertical coordinate

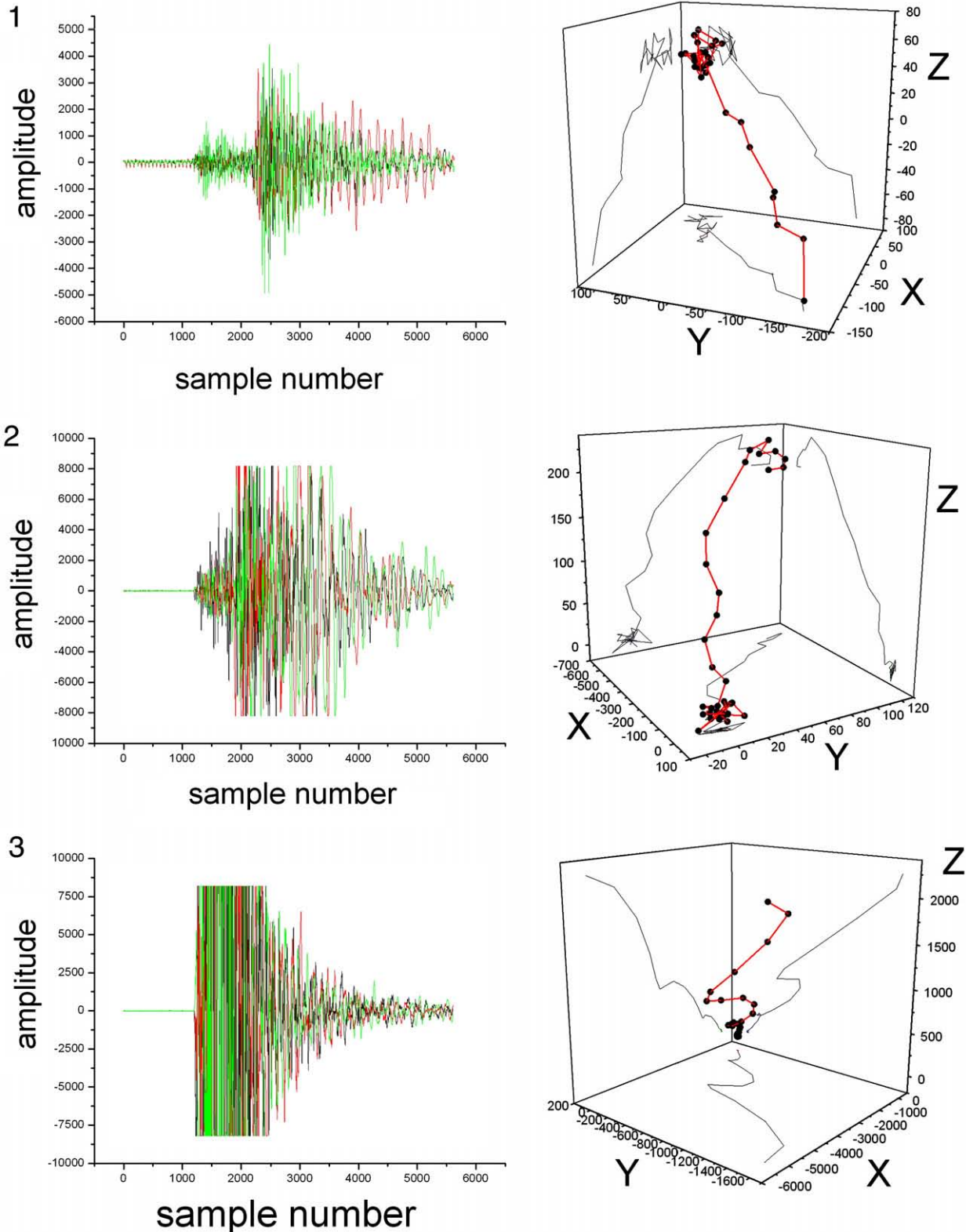


Fig. 11. Waveforms of the event number 272 (Table 1) recorded by the three triaxial geophones (left column) and trajectory of particle motion at onsets of the P-waves.

location error is unacceptably high (Fig. 7A), which is probably due to the effect of the “flat” array, typical for the P-wave first arrival time location method. This is well known that hypocenter location with P arrivals alone leads to large errors in the estimation of depth (Mendecki, 1997).

The directional location method behaves in the opposite way. The hypocenter vertical coordinate error is small (Fig. 8A) but the epicenter location error is very high (Fig. 8B).

The combined methods (Figs. 9 and 10) were developed in order to “merge” the merits of the P-wave arrival algorithm and directional algorithm. For both of combined methods the epicenter and vertical coordinate of the hypocenter errors are smaller compared to the first and the second methods (particularly for the two-step method). The time needed for evaluation of the error map is significantly shorter for the two-step algorithm than for the combined misfit function algorithm. Consequently, we have chosen the first algorithm to perform location of mine tremors in LCM.

A typical seismic event recorded by a small array of triaxial geophones is presented in Fig. 11. For each geophone the particle motion trajectory for P-wave onset is also shown. For most signals, this part of the three component signal is linearly polarized and can be used for the estimation of the direction of P-wave propagation.

A part of the three component signal near a typical P-wave onset is presented in Fig. 12. P-wave onset can be precisely extracted when the energy of noise is low. In case of presence of highly contaminated records the onset determination may contain a significant error. The extraction was done by approximation of the particle motion trajectory by a straight line at the moment of its first break. The interval used during the seismogram interpretation is marked in Fig. 12 with two vertical lines. We have used a rather short interval, usually less than one quarter of the wave period. The discrete trajectory (marked by black dots) approximated by a straight line is shown in Fig. 13.

Having the P-wave onsets extracted from all geophones and directions of the P-waves on triaxial geophones it was possible to use the two-step algorithm to locate the recorded tremors in

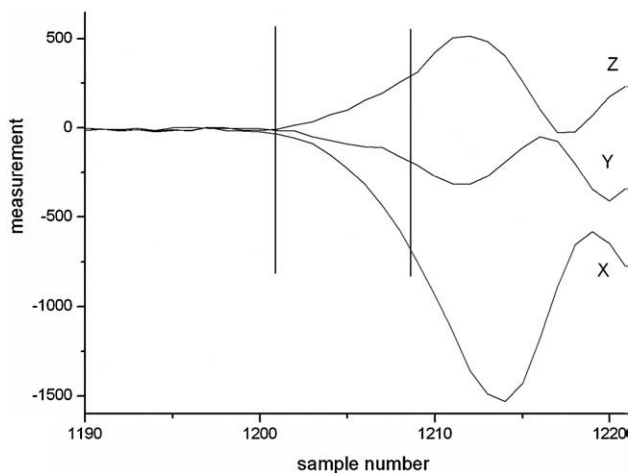


Fig. 12. Waveforms recorded by X, Y and Z components of triaxial geophone near the P-wave onset. The interval used for the direction’s estimation is shown by two vertical lines.

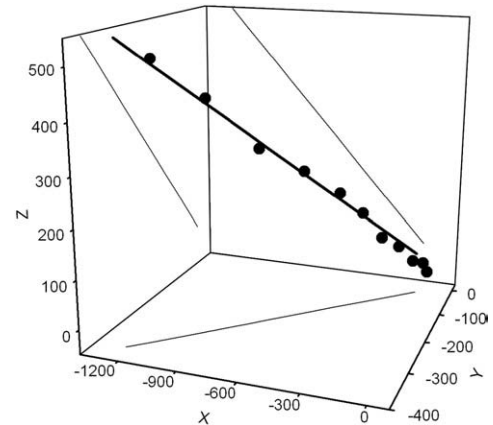


Fig. 13. A particle motion trajectory near the P-wave onset. A straight line approximates the particle motion trajectory in case of linear polarization.

observed area. In Table 1 we present locations of real tremors from LCM, located by the two-step combined algorithm described in this work in panel G6/X/9 and the adjacent panel G6/X/10 (located on south). Contrary to the P-wave time arrival algorithm, it allowed to estimate the vertical hypocenter coordinate correctly (with an acceptable location error). Additionally for the small triaxial array the two-step algorithm allows to estimate the epicenter of tremor much more precisely than the directional algorithm.

Table 1
Example results of location of the mine tremors from Lubin Copper Mine (LCM) inside and in the vicinity of panel G6/X/9

Id	Date	Time	Panel	Energy	Located hypocenter coordinates			Depth error
					X [m]	y [m]	z [m]	
272	2005-01-04	6:11:46	G6/X/10	1.1E5	26,217	9757	-602	74
468	2005-01-14	19:2:5	G6/X/9	2.9E4	26,747	9767	-550	61
624	2005-01-28	5:41:11	G6/X/9	2.4E5	26,757	9722	-480	78
639	2005-01-29	12:43:31	G6/X/9	2.4E4	26,600	9653	-572	39
691	2005-02-02	9:41:47	G6/X/10	1.6E4	26,678	9744	-540	31
861	2005-02-14	2:35:44	G6/X/9	3.6E4	26,421	9844	-449	74
889	2005-02-16	14:54:3	G6/X/9	8.0E3	26,232	9766	-601	107
912	2005-02-18	19:35:35	G6/X/9	1.1E4	25,505	9095	-288	143
997	2005-02-23	15:31:57	G6/X/10	1.1E4	26,754	9735	-580	32
1002	2005-02-24	1:27:39	G6/X/9	4.3E3	26,805	9981	-610	23
1388	2005-23-40	5:23:40	G6/X/9	5.2E3	26,889	9840	-664	15
1404	2005-03-27	5:5:46	G6/X/9	2.5E4	26,827	9999	-708	70
1612	2005-04-12	12:51:29	G6/X/9	1.9E3	26,997	9982	-509	50
2160	2005-05-11	19:20:17	G6/X/9	1.7E4	2505	9635	-252	88

It is possible to check the location results directly only for the tremors that occurred close to the mining panel and their effects are visible during mine openings. Because their real location are known they can be compared with the locations obtained by the proposed algorithm. For example, the service at the LCM seismological station confirmed the positive locations of the tremors numbered 272 and 889. Both tremors were located close to the excavation and cause the visible damage to the underground equipment (broken supports, crushed cutting machines) and constructions (destroyed roofs and roof bolting). For the others tremors shown in Table 1, the real hypocenters coordinates were not known.

5. Summary

The presented two-step combined location method is currently used in LCM to locate mine tremors, employing location by P-waves first arrival times and P-waves directions. In the case of LCM, the data for the combined location procedure are taken from completely independent arrays of geophones.

By numerical Monte-Carlo experiments the location error maps has been constructed. The designed error propagation algorithm is fully non-linear and does not suffer from the problems induced from the linearization problem, such as high error location values close to geophones. The evaluated maps demonstrate the positive features of the combined method of source location. The most important one is the high vertical resolution of the combined array, which was the main task of the realized project in LCM.

There are also additional advantages for this method. The directional stage of the location procedure is much faster than the classical P-wave arrival time algorithm. After the directional stage of the combined algorithm, the dimension of the surveyed space of possible locations is decreased (vertical component of the hypocenter is already determined). Thus the P-wave arrival time algorithm can be used to search only for the epicenter position, which significantly reduces computational time. The presented combined method is fast for the multilayered rock mass model and can be used by a single computer at a seismological station. For more complex rock mass models it can be

applied only when a parallel computing environment can be used.

We believe that presented location method can be easily introduced into mines where the accuracy of the vertical hypocenter coordinate location needs to be increased. Installing merely a few of triaxial geophones in an interesting area can greatly raise the vertical location precision. As the additional triaxial array can be completely independent from the existing one, the installation should not be expensive and technically difficult.

Acknowledgments

We thank the anonymous reviewers for their valuable comments that helped us to improve the presentation of this paper. The research has been funded under grant 4 T12B 042 28 by the Polish government.

References

- Horst, R., Pardalos, P.M., 1995. Handbook of Global Optimization. Kluwer Academic Publishers, London.
- Jackson, G.M., Mason, I.M., Greenhalgh, S.A., 1991. Principal components transforms of triaxial recordings by singular value decomposition. *Geophysics* 56 (4), 528–533.
- Jurkasevics, A., 1988. Polarization analysis of three-component array data. *Bull. Seismol. Soc. Am.* 78 (5), 1725–1743.
- Lee, W.H.K., Stewart, S.W., 1981. Principles and Applications of Micro-earthquake Networks. Adv. Geophys. Academic Press, San-Diego.
- Mendecki, A.J., 1997. Seismic Monitoring in Mines. Chapman & Hall, London.
- Pavlis, G.L., Vernon, F., Harvey, D., Quinlan, D., 2004. The generalized earthquake-location (GENLOC) package: an earthquake-location library. *Comput. Geosci.* 30, 1079–1091.
- Press, W.H., Flannery, B.P., Teukolsky, S.A., Vetterling, W.T., 1986. Numerical recipes in C. The art of scientific computing. Cambridge University Press, Cambridge.
- Pszczoła, G., Leśniak, A., 2004. Non-linear optimization methods for small earthquake locations. *T.A.S.K. Q.* 8 (4), 583–590.
- Samson, J.C., 1977. Matrix and Stokes vector representation of detectors for polarized waveforms: theory with some application to teleseismic waves. *Geophys. J. R. Astr. Soc.* 51, 583–603.
- Wagner, G.S., Owens, T.J., 1996. Signal detection using multi-channel seismic data. *Bull. Seismol. Soc. Am.* 86 (1A), 221–231.